



Cryo X-ray Absorption Spectroscopy of Copper Zinc Tin Sulfide Nanoparticles

Rein, Christian; Ramos, Tiago; Andreasen, Jens Wenzel

Publication date:
2019

Document Version
Publisher's PDF, also known as Version of record

[Link back to DTU Orbit](#)

Citation (APA):

Rein, C., Ramos, T., & Andreasen, J. W. (2019). *Cryo X-ray Absorption Spectroscopy of Copper Zinc Tin Sulfide Nanoparticles*. Poster session presented at DanScatt Annual Meeting 2019, Aarhus, Denmark.

General rights

Copyright and moral rights for the publications made accessible in the public portal are retained by the authors and/or other copyright owners and it is a condition of accessing publications that users recognise and abide by the legal requirements associated with these rights.

- Users may download and print one copy of any publication from the public portal for the purpose of private study or research.
- You may not further distribute the material or use it for any profit-making activity or commercial gain
- You may freely distribute the URL identifying the publication in the public portal

If you believe that this document breaches copyright please contact us providing details, and we will remove access to the work immediately and investigate your claim.

Cryo X-ray Absorption Spectroscopy of Copper Zinc Tin Sulfide Nanoparticles.

Christian Rein*, Tiago Ramos & Jens Wenzel Andreasen.
DTU Energy, Technical University of Denmark, Risø, Denmark. *chrr@dtu.dk

X-ray absorption spectroscopy (XAS) is used to probe the atomic environment in quaternary compounds, like the earth abundant and non-toxic $\text{Cu}_2\text{ZnSnS}_4$ (CZTS) absorber material (Fig. 1) used in 3rd generation solar cells¹. Cooling the structure down to 100 K decreases thermal fluctuations and improves XAS data quality for an improved FEFF-based fitting (Fig. 2 & 3).

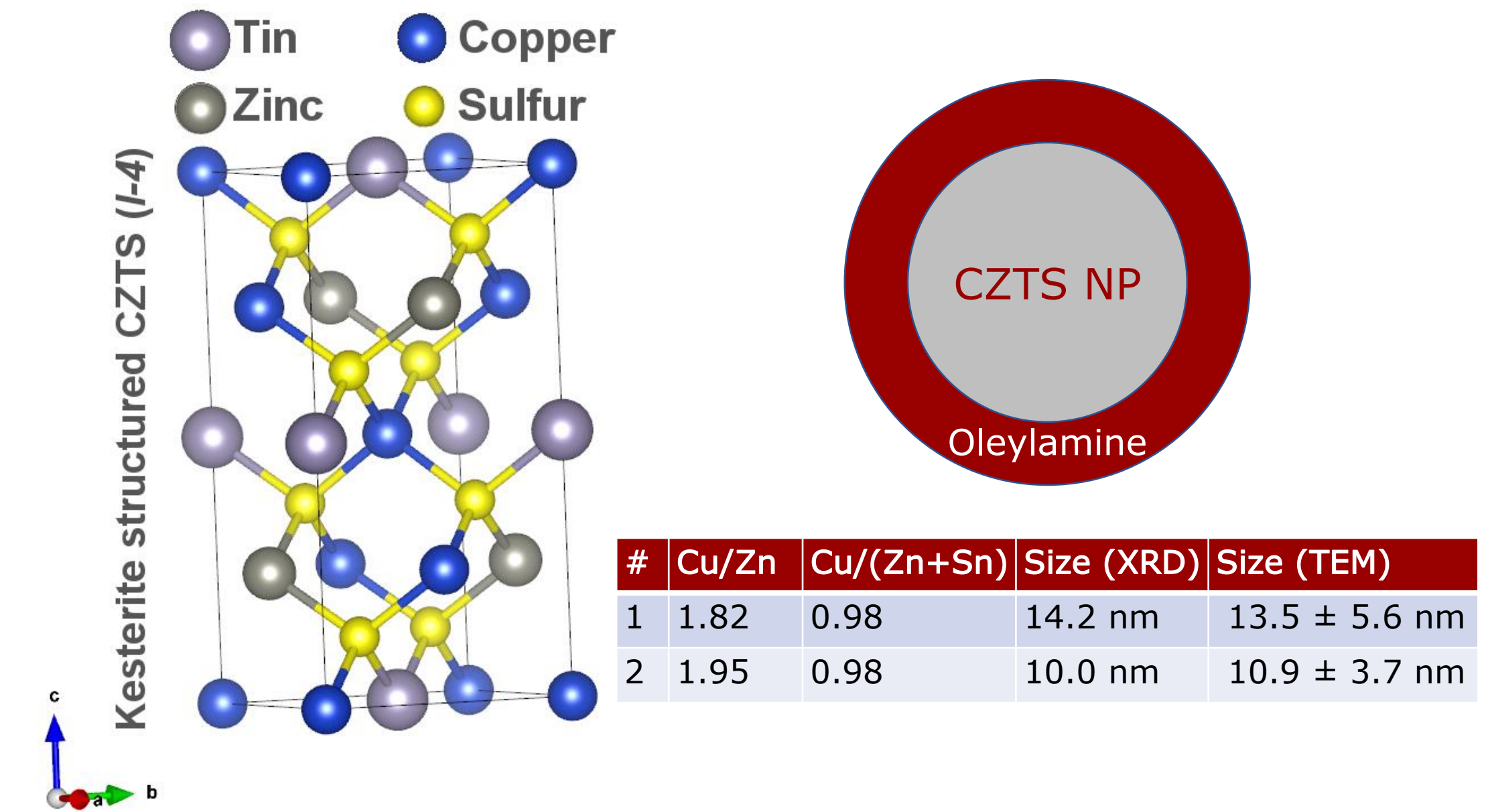


Figure 1: Left, CZTS unit cell structure. Top Right, CZTS nanoparticle (NP) with organic (Oleylamine) ligand capping. Bottom right, average composition (from EDX) and size distribution of CZTS NPs.

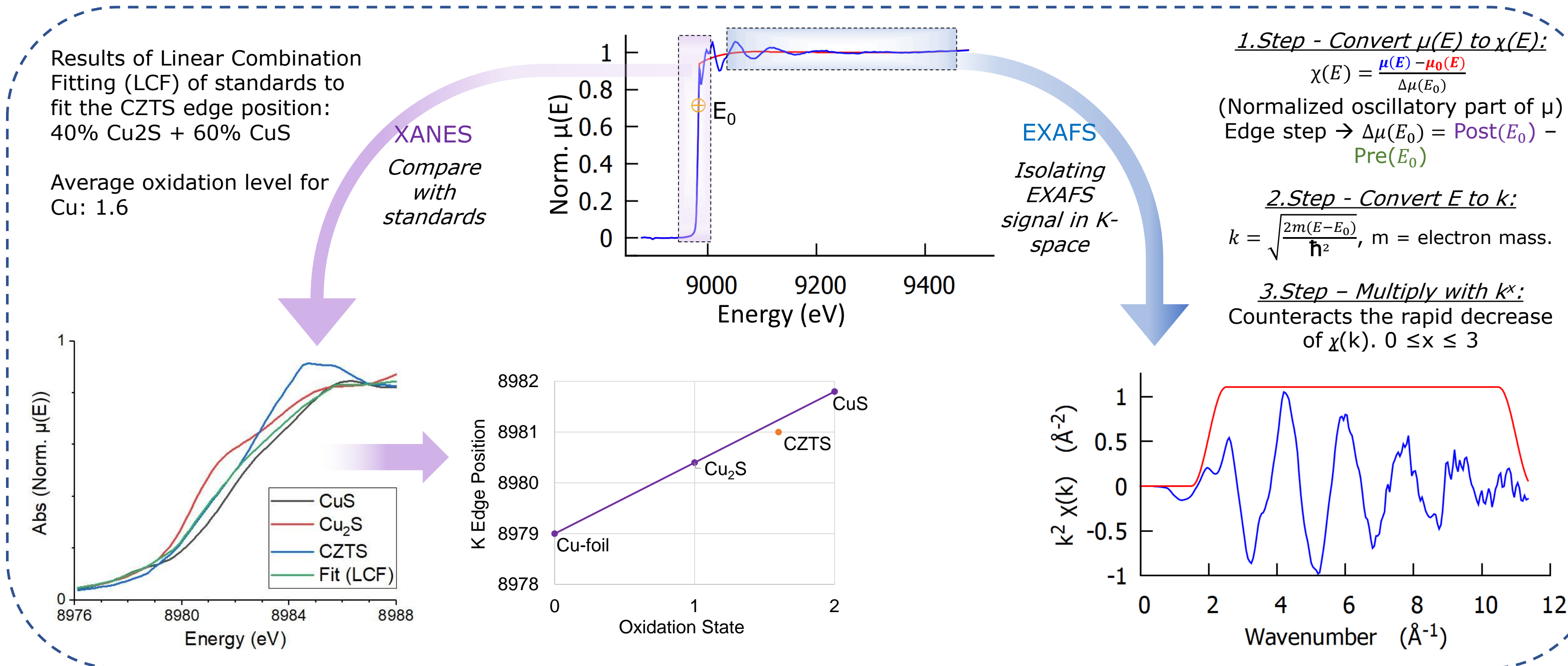


Figure 2: XAS data analysis can be divided into XANES and EXAFS analysis. XANES analysis can indicate oxidation level of the probed element (here Cu) by using Linear Combination Fitting (LCF) of known standard sample data. An oxidation level for Cu of 1.6 is obtained for such fitting to CZTS XANES data. EXAFS analysis begins by isolating the absorption modulation signal further (>30 eV) from the edge (E_0). Based on the Signal/Noise a fitting window (red curve) is applied to the data in k-space before converting to radial-space (R-space) for evaluation of neighbor distances.

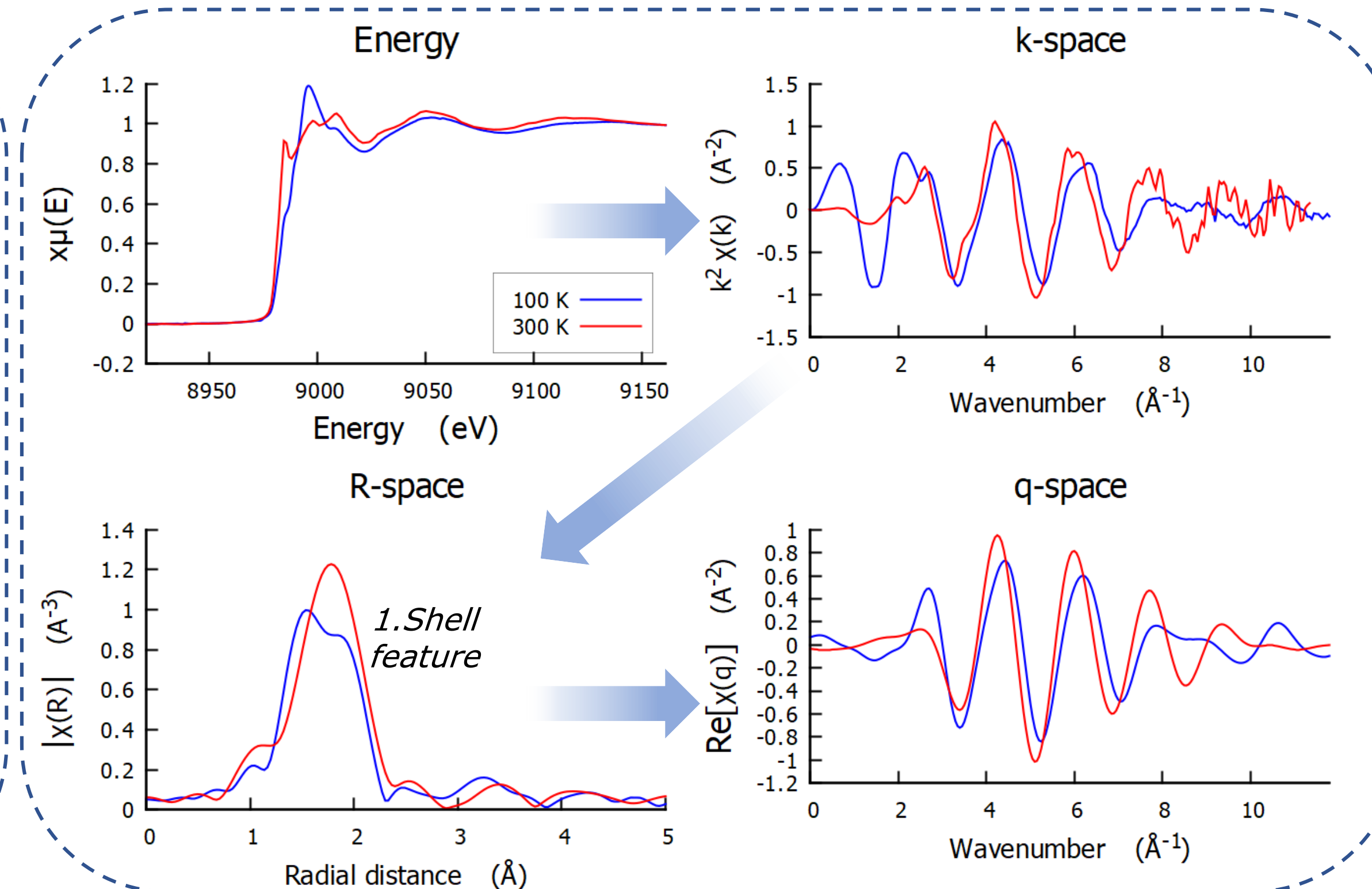


Figure 3: Cu-edge EXAFS analysis of sample #1 at 100 K and 300 K. The isolated signals in k-space (2.5-11.8 \AA^{-1}) was Fourier transformed (FT) to indicate trends in radial distance (R-space). A splitting and shortening of R for the 1. shell feature is observed when cooling down to 100 K. Inverse FT of a select R-space (1.3-4.0 \AA) to q-space, simulates the most important features in k-space. These ranges is implemented in a FEFF-fitting routine.

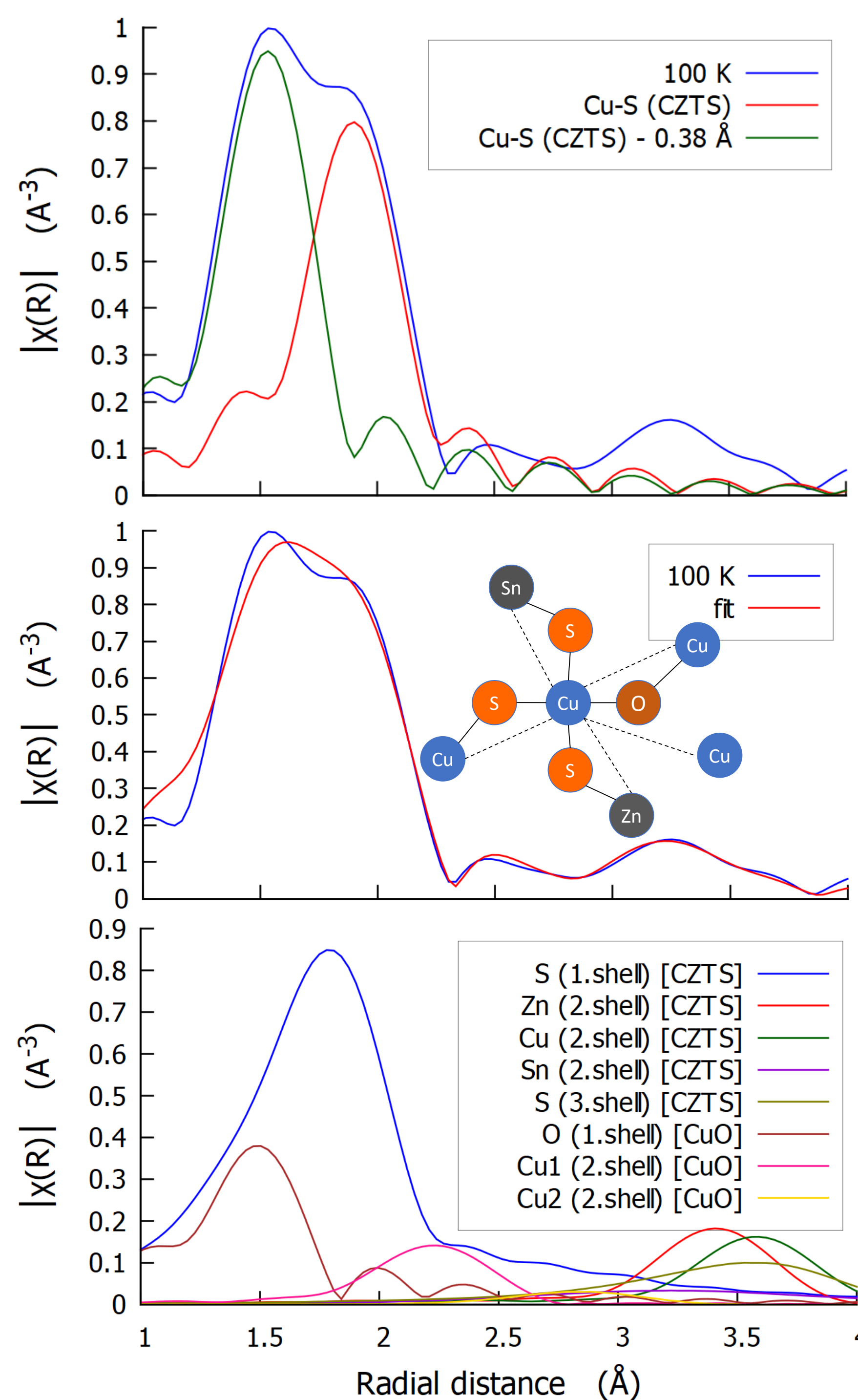
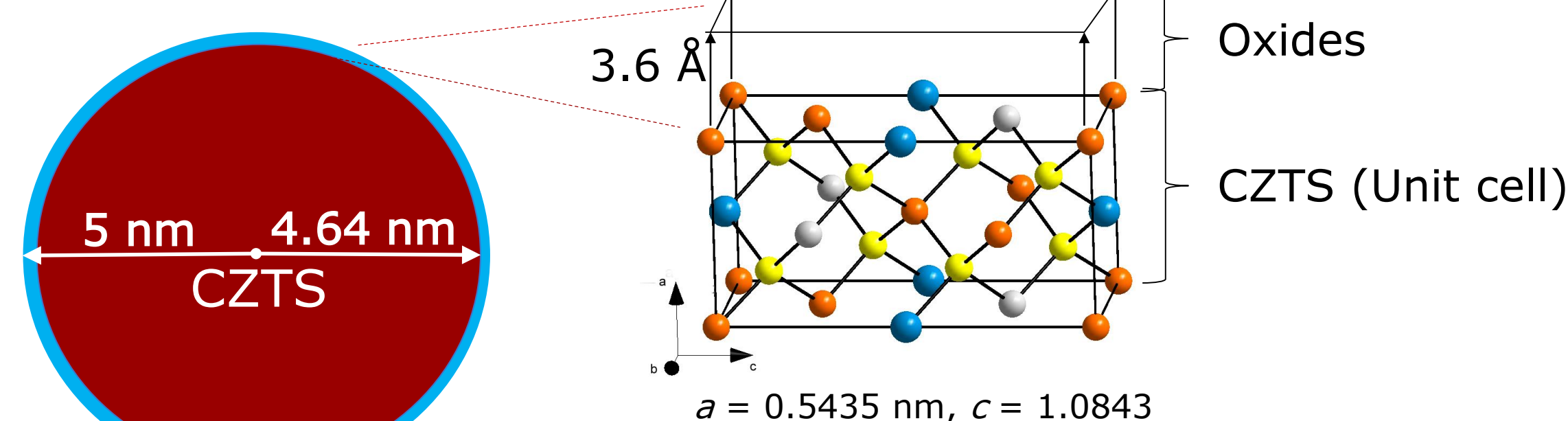


Figure 4: Cu-edge EXAFS analysis for CZTS at 100 K. Top, dual peak 1. shell feature. Middle, FEFF-fitting including both CZTS and CuO structure. The FEFF-software calculates the effective amplitudes ($|f_{\text{eff}}|$), total scattering phase shift and other parameters of the individual scattering paths. Bottom, Scattering contributions to the FEFF-fit from the individual scattering atoms.

Cryo-EXAFS analysis indicates two different neighbors to Cu-atoms (Fig. 4, top). The shortest radial distance can be simulated by a 16% bond shortening of the Cu-S bond ($2.33 \text{ \AA} \rightarrow 1.95 \text{ \AA}$). But cooling have previously been observed to change only <1% in bond length², which indicate other factors must be causing the deviation.

An oxidized CZTS shell:

Only by replacing a fraction of the Cu-S bonds in the model of CZTS with the shorter Cu-O bonds (CuO: 1.963 \AA) can a reasonable (R-factor = 0.01) fit to the EXAFS signal be obtained (Fig. 4, middle and bottom). In the fit, scattering amplitudes related to the oxide are set to proportionally reduce the scattering amplitudes of those related to CZTS, which allow us to assess the degree of oxidation (Fig. 5). Similarly for Zn- and Sn-edge EXAFS, dual peak 1. shell features are observed, which can be partly fitted with oxide products (Fig. 6). XPS analysis of similar CZTS compound have also revealed a 15.2 % oxidation of CZTS. A 20 % oxidation of the CZTS NP would be equivalent with the formation of a 3.6 \AA oxide shell around the 10 nm diameter CZTS NP. Nitrogen bonds from the ligand capping could also contribute to the deviations, but their effect is difficult to distinguish from that of oxygen.



Scatter atom	r (Å)	Δr (Å)	σ^2	Amplitude	Fraction
S (1. shell)	2.330	-0.072	0.0117	0.595	82 % CZTS
Zn (2. shell)	3.837	-0.091	0.0123		
Cu (2. shell)	3.837	0.093	0.0124		
Sn (2. shell)	3.842	-0.386	0.0604		
S (3. shell)	4.501	-0.275	0.0294		
O (1. shell)	1.955	-0.046	0	0.132	18 % CuO
Cu1 (2. shell)	2.897	-0.337	0.0100		
Cu2 (2. shell)	3.081	0.142	0.0189		

Figure 5: FEFF-fitted parameters for the Cu-edge EXAFS data at 100 K. Literature values of bond distances (r) can be grouped into "shells" that have similar R-space features. The amplitude from the scattering atom is reduced by r and an additional amplitude factor is applied depending on whether the structure is CZTS (top group) or CuO (bottom group).

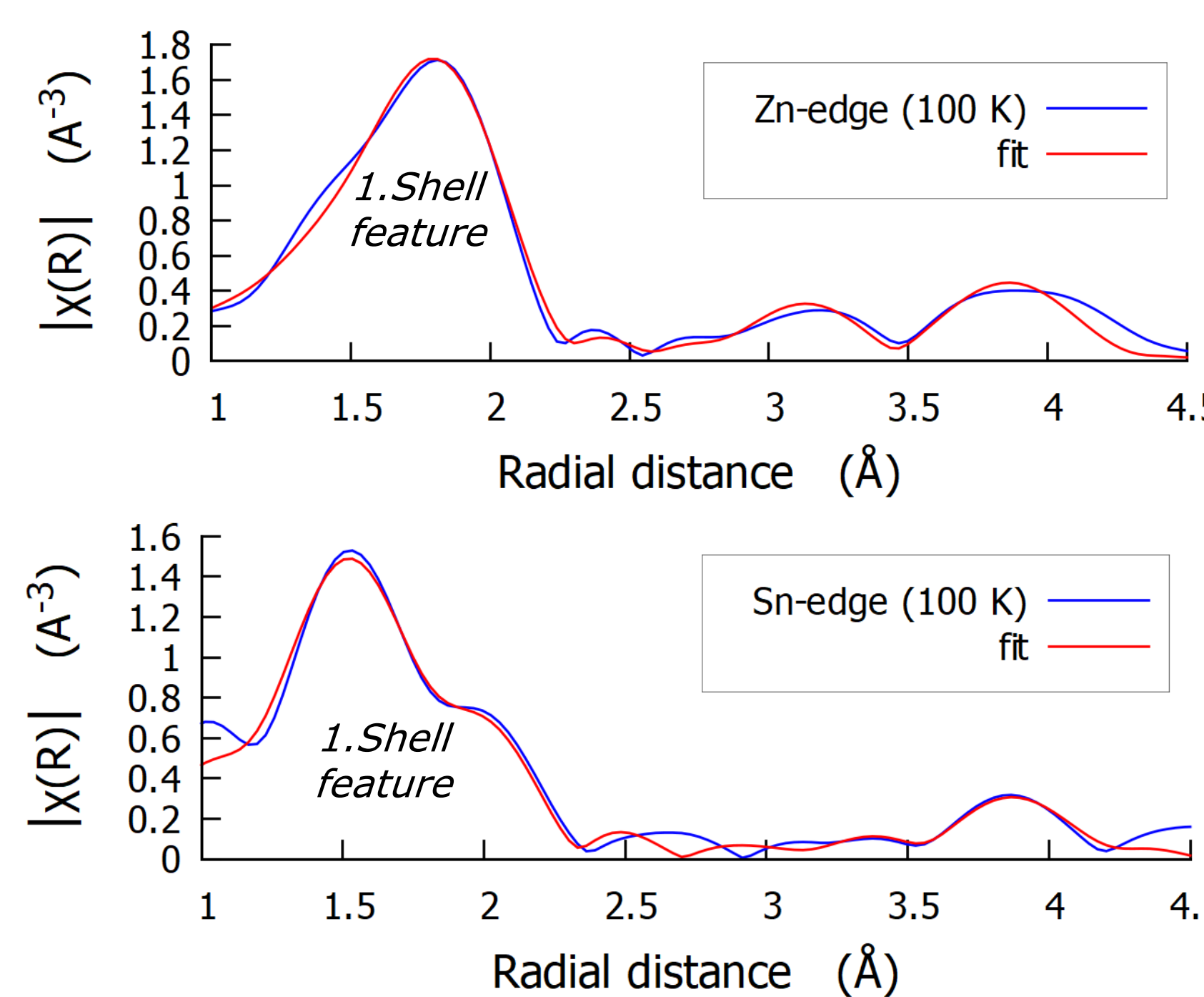


Figure 6: FEFF-models for Zn- (top) and Sn- (bottom) EXAFS data. 22% ZnO was included in the model for Zn-edge EXAFS and 25 % SnO_2 of Sn-edge EXAFS, but data quality for Sn in k-space was low, which makes the fitted oxide fraction less reliable than for Cu- and Zn-edge EXAFS data.